VIP High-Field Pulsed EPR Spectroscopy

DOI: 10.1002/anie.200703753

Structure of the Tyrosyl Biradical in Mouse R2 Ribonucleotide Reductase from High-Field PELDOR**

*Vasyl P. Denysenkov, Daniele Biglino, Wolfgang Lubitz, Thomas F. Prisner, and Marina Bennati**

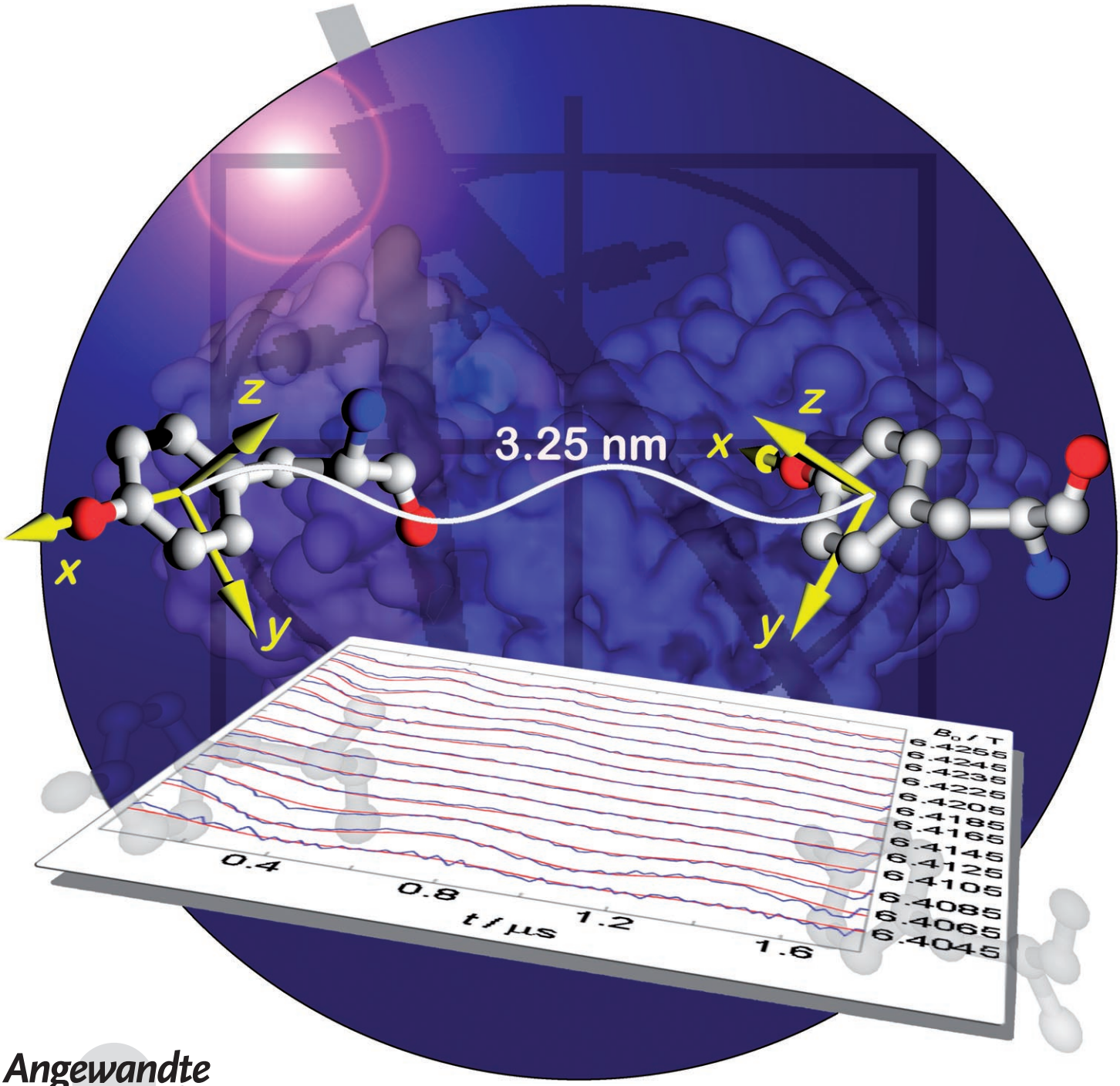

Ribonucleotide reductase (RNR) is a target enzyme for cancer chemotherapy and antiviral agents.[1–3] Structural studies of RNR from different organisms can provide fundamental information to develop new drugs. In this respect, the mammalian mouse RNR serves as a model for human RNR. Almost all eukaryotic organisms encode class I RNRs and are composed of two subunits, R1 and R2. The R2 subunit contains the essential diferric cluster tyrosyl radical (Y•) cofactor, and R1 is the site of the conversion of nucleoside diphosphates into 2′-deoxynucleoside diphosphates.[4,5] It has been proposed that the function of the tyrosyl radical in R2 is to generate a transient thiyl radical in R1 over a distance of 35 Å, which in turn initiates the reduction process.[6,7] In the class I RNR from mouse, the X-ray structure of R2 has been solved only in the monomeric form and at pH values far from physiological conditions.[8,9] Biochemical studies[10] have revealed that the active form of mouse RNR has a $(R1)_2(R2)_2$ or $(R1)_6(R2)_6$ structure. Recent pulse electron–electron double resonance (PELDOR) experiments[11] on mouse R2 reconstituted in vitro led to detection of a single Y• interradical distance of 3.25 nm. In the study reported herein we employ PELDOR at high microwave frequencies[12–15] to experimentally assess the homodimeric structure of the active protein in solution. We use the essential Y• radicals as spin probes to detect their distance and mutual orientation and present a general approach to analyze the data. This work demonstrates for the first time the capability of this method to construct a biradical structure when the crystal structure is not available. This method has considerable potential for studying the assembly of protein complexes in which paramagnetic centers are rigidly embedded.

PELDOR detects weak dipolar interactions between radicals and is based on a two-frequency pulse sequence.[16–18] One frequency is required to select the detected radical spins and the second one to perturb the coupled partner spins. The perturbation causes a change in the dipolar field of the detected spin and results in a modulation of the time-domain spin-echo signal as a function of the dipolar frequency. The distance information is encoded in the observed dipolar frequency and can be determined in experiments at low fields (9 GHz EPR). At high magnetic fields the EPR spectra are dominated by the anisotropy of the g tensors,[19] and the PELDOR effect becomes also a function of the mutual radical orientation. The structure of the biradical, defined by the orientation of the g tensors with respect to the interconnecting distance vector (Figure 1), is obtained from analysis of

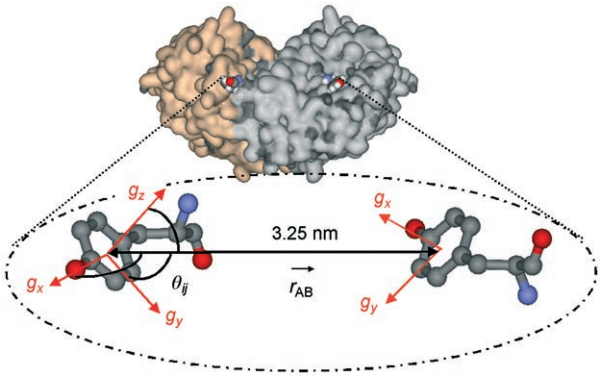

Figure 1. The RNR R2 dimer from mouse. Structure of the tyrosyl biradical as defined by the projection angles θ_{ij} between the g-tensor principal axes and the dipolar distance vector $\boldsymbol{r}$ at each radical site; top: space-filling docking model from the X-ray monomer structure as proposed by Strand et al.[9] (see also PDB entry 1W68).

the PELDOR response at different field positions in the EPR line,[13] that is, at different orientations of the magnetic field with respect to the g-tensor principal axes. We illustrate in this work that the analysis of the traces can be performed a priori provided that the signal-to-noise ratio is large enough and the data pattern delivers enough constraints to construct the biradical structure.

Figure 2 illustrates 180 GHz PELDOR modulation traces of a 0.2 mM mouse R2 (1.6 Y• per R2) sample after subtraction of the echo decay. The state of the sample was the same as previously reported in reference [11]. The data were recorded across the EPR line from $B \parallel g_z$ to $B \parallel g_x$. In the stack plot the

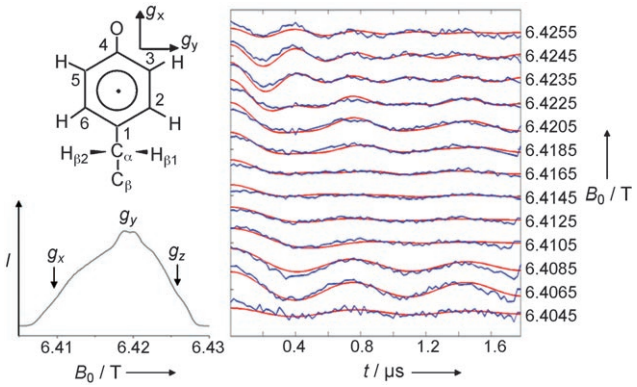

Figure 2. Right: Blue lines show 180 GHz orientation-dependent PELDOR traces recorded across the EPR line from $B \parallel g_z$ (top) to $B \parallel g_x$ (bottom); red lines show the best global fit with the parameters given in Table 1. Left, top: Structure of the tyrosyl radical. The directions of the g-tensor principal axes are collinear with the molecular axes. Left, bottom: 180 GHz echo-detected EPR spectrum of the tyrosyl radical in mouse R2.

[*] Dr. M. Bennati
Max Planck Institute for Biophysical Chemistry
Göttingen (Germany)
Fax: (+49) 551-201-1467
E-mail: bennati@mpibpc.mpg.de
Homepage: http://www.mpibpc.gwdg.de/groups/bennati

Dr. V. P. Denysenkov, Prof. T. F. Prisner
Institute of Physical and Theoretical Chemistry and BMRZ
University of Frankfurt, Frankfurt (Germany)

Dr. D. Biglino, Prof. W. Lubitz
Max Planck Institute for Bioinorganic Chemistry
Mülheim an der Ruhr (Germany)

[**] We thank P. P. Schmidt for helping with the sample preparation and Prof. Lars Thelander (Umeå, Sweden) for supplying us with *E. coli* cells that overexpress mouse R2 protein. M.B. would like to acknowledge the Max Planck Society and the IRTG 1422 for financial support. PELDOR = pulse electron–electron double resonance.

amplitudes were scaled with respect to the maximal observed amplitude to account for the observed modulation depth. The frequency difference between pump and detection was kept constant to $\Delta\nu = 60$ MHz. The traces show a clear field dependence in the modulation frequency as well as in the damping and in the modulation depth. The pattern displays the frequency $\nu_{\parallel}$ of the dipolar tensor[11] occurring at field positions between g_z and g_y and the frequency $\nu_{\perp}$ at fields parallel to g_x. This indicates that the x axis of the g tensor, located along the C–O bond of Y· (Figure 2 inset), is close to the normal of the unique z axis of the dipolar tensor. The most peculiar features are encountered in the spectral range between g_y and g_z. It is evident that at least two frequencies contribute in this region. Furthermore, the orientation selection is strongly dependent on the size of the hyperfine couplings, and precise information can be obtained only from spectral simulations. A second set of data for $\Delta\nu = 100$ MHz (not shown) was recorded and displayed an overall similar appearance as the data in Figure 2. Nevertheless, some differences in the modulation depth and in the spectral damping were found and used to provide additional constraints in the following analysis.

The data in Figure 2 were analyzed with a fit procedure reported previously.[13] However, we discuss now the geometrical problem without any symmetry restriction. The mutual orientation of two radicals can be generally expressed by a rotation from the g tensor of radical 1 to the g tensor of radical 2 characterized by three Euler angles α, β, γ. The axially symmetric dipolar tensor can be related to either one of the g tensors by a rotation with only two Euler angles. This results in a total of five angular parameters for the computation of the PELDOR frequencies. To obtain fit results that can be easily interpreted as structural parameters, we express the g-tensor orientations through two consecutive rotations, $\boldsymbol{R}_\mathbf{d}$ and $\boldsymbol{R}'_\mathbf{d}$, using the dipolar tensor as a common frame (Figure 3). Within this definition, $\boldsymbol{R}_\mathbf{d}$ and $\boldsymbol{R}'_\mathbf{d}$ contain the direction cosines and thus the projection angles θ_{ij} between the g axes and the dipolar vector $\boldsymbol{r}$[20] (Figure 1).

All principal values of the g,[21] A,[22] and D[11] tensors were known from previous EPR experiments, as reported in Table 1. To fit the data, we tested several arbitrary starting sets of orientations, and the solution consistently converged into a minimum. This minimum had a width in parameter space of about 10°, that is, we found within 10° several combinations of values for the five Euler angles that delivered similar fit qualities. We report in Table 1 one representative solution. From the obtained projection angles θ_{ij} (Table 1) for radical 1 and radical 2 we note that both g tensors display a similar orientation with respect to the dipolar vector, and the solution represents a biradical with the radicals oriented in an almost antiparallel fashion. This solution is consistent with the orientation predicted by the docking model of the monomer X-ray structures (Figure 1). For some starting parameter sets we also found a second solution which is symmetry-related to the first one, that is, with the two radicals aligned in a parallel fashion (both g_x axes pointing in the same direction). However, this solution would be incompatible with any docking model of the protein. Since the Y· radicals are well oriented within the protein and distributions in the local environment of the Y· radicals have never been reported for the same organism, we conclude that our result is consistent with a homodimeric protein structure.

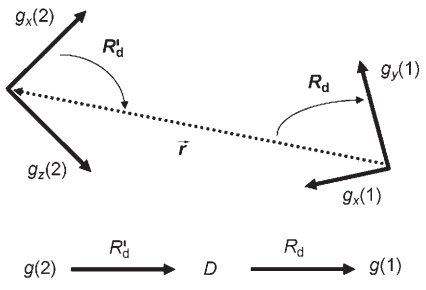

Figure 3. Frame transformations in a biradical; g and D denote the frames of the g and dipolar tensor, respectively. The frame rotation $D \rightarrow g(1)$ is $\boldsymbol{R}_\mathbf{d}$ and is defined by only two Euler angles, whereas the second rotation $g(2) \rightarrow D$, denoted $\boldsymbol{R}'_\mathbf{d}$, requires consequently three angles.[20]

Table 1: Rotation matrices and orientations for the Y· radical pair in the RNR R2 dimer from mouse.

	α [°]	β [°]	γ [°]
$\boldsymbol{R}_\mathbf{d}$	0	44	80
$\boldsymbol{R}'_\mathbf{d}$	−68	144	−145
$\theta(1)$[a](g_i/r)	97	47	44
$\theta(2)$[b](g_i/r)	103	57	36
θ[c](g_i/r)	97	59	32

[a] Projection angles between the x, y, and z axes (g_i) of the g tensor (radical 1) and the dipolar vector $\boldsymbol{r}$ from matrix $\boldsymbol{R}_\mathbf{d}$. [b] Projection angles for radical 2 from matrix $\boldsymbol{R}'_\mathbf{d}$.[20] [c] Projection angles for the symmetric biradical structure of *E. coli* R2 from reference [13]. The following tensor principal axis values (x, y, z) were used to simulate the EPR line: g: 2.0076, 2.0043, 2.00225; $A_{\text{H-}\beta1}$: 2.07, 1.88, 1.87 mT; $A_{\text{H-}3,5}$: −0.90, −0.25, −0.69 mT. $D_{\parallel} = -2\ D_{\perp}$: −2.9 MHz. The Euler angles (α, β, γ) are defined in a left-handed coordinate system for counterclockwise rotations around z, y', z'' (in that order). The primes denote the new coordinate systems generated after each rotation.

In Table 1 we compare the obtained orientations with the ones reported for *E. coli* R2.[13] We find that the orientations of g_x with respect to $\boldsymbol{r}$ are similar within the estimated experimental error of ±5°, whereas the orientations of g_y and g_z differ slightly. Small local structural differences in the environment of Y· were previously reported in several EPR studies. ENDOR experiments[23] had demonstrated that the radical in mouse R2 is hydrogen-bonded, likely to a water molecule. The H bond is absent in the *E. coli* Y· radical. This difference is also reflected in the g_x values, which are very sensitive to the electrostatic environment.[21,24,25] Secondly, the hyperfine coupling to the H_β protons in the tyrosyl side chain is related to the dihedral angle defined by the tyrosyl ring plane, the C_β atom, and the position of C_α in the plane containing C_α and the H_β protons.[26] Different hyperfine couplings for the H_β protons were reported in ENDOR[22] and high-field EPR studies.[27] Quantum chemical calculations[24,25] predicted that the observed hyperfine couplings in Y· from *E. coli* are consistent with a dihedral angle of 38–40°, whereas the couplings in Y· from mouse (Table 1) are consistent with an angle of 30°. This results in a difference

between the dihedral angles of about 10° and can be rationalized by a small reorientation of the radical around the g_x axis. The size of this reorientation is consistent with the small displacement observed in our PELDOR results.

In summary, the 180 GHz PELDOR traces on the tyrosyl radicals in R2 from mouse RNR show pronounced orientational selectivity, which could be employed to determine the biradical structure. Analysis of the traces resulted in an almost symmetric biradical structure. Since the tyrosyl radicals are well oriented within the protein, the symmetric biradical is consistent with a homodimeric protein structure. The small differences found by comparison of the *g*-tensor orientations with R2 from *E. coli* are consistent with local structural differences at the radical site, as previously reported by EPR and ENDOR data. Our results demonstrate that the construction of a biradical structure is feasible from high-field PELDOR data and the method can be used to study the relative orientation of protein complexes, if suitable paramagnetic probes are available.

Experimental Section

The protein R2 from mouse was prepared as described in reference [11]. 180 GHz PELDOR spectroscopy was performed with a home-built 180 GHz pulsed EPR spectrometer extended for two-frequency irradiation.[12] The pumping frequency was set at a constant offset from the detection frequency. The set of experiments consisted of several traces recorded at different fields across the EPR spectrum, in steps of 20 Gauss from $B \parallel g_x$ to $B \parallel g_y$ and in steps of 10 Gauss from $B \parallel g_y$ to $B \parallel g_z$. The duration of the pumping pulse was adjusted to about 80 ns, and the detection pulses were approximately 30 and 60 ns. The four-pulse, dead-time free DEER (double electron–electron resonance spectroscopy) sequence was employed using a time window of 2 μs between the second and third pulses and a pulse sequence repetition time of 100 ms at a temperature of 5 K. The intrinsic echo decay was eliminated from the modulation trace by fitting an exponential or polynomial function to the traces and dividing the experimental data by the fitted function.

Received: August 15, 2007
Revised: October 8, 2007
Published online: January 2, 2008

Keywords: EPR spectroscopy · PELDOR spectroscopy · radicals · ribonucleotide reductase · structure elucidation

[1] J. Stubbe, W. A. van der Donk, *Chem. Biol.* **1995**, *2*, 793 – 801.
[2] C. R. Kowol, R. Berger, R. Eichinger, A. Roller, M. A. Jakupec, P. P. Schmidt, V. B. Arion, B. K. Keppler, *J. Med. Chem.* **2007**, *50*, 1254 – 1265.
[3] E. Torrents, M. Sahlin, D. Biglino, A. Gräslund, B.-M. Sjöberg, *Proc. Natl. Acad. Sci. USA* **2005**, *102*, 17946 – 17951.
[4] A. Jordan, P. Reichard, *Annu. Rev. Biochem.* **1998**, *67*, 71 – 98.
[5] H. Eklund, U. Uhlin, M. Färnegårdh, D. T. Logan, P. Nordlund, *Prog. Biophys. Mol. Biol.* **2001**, *77*, 177 – 268.
[6] J. Stubbe, W. A. van der Donk, *Chem. Rev.* **1998**, *98*, 705 – 762.
[7] J. Stubbe, D. G. Nocera, C. S. Yee, M. C. Y. Chang, *Chem. Rev.* **2003**, *103*, 2167- 2201.
[8] B. Kauppi, B. B. Nielsen, S. Ramaswamy, I. K. Larsen, M. Thelander, L. Thelander, H. Eklund, *J. Mol. Biol.* **1996**, *262*, 706 – 720.
[9] K. R. Strand, S. Karlsen, M. Kolberg, Å. K. Røhr, C. H. Görbitz, K. K. Andersson, *J. Biol. Chem.* **2004**, *279*, 46794 – 46801.
[10] O. B. Kashlan, B. S. Cooperman, *Biochemistry* **2003**, *42*, 1696 – 1706.
[11] D. Biglino, P. P. Schmidt, E. J. Reijerse, W. Lubitz, *Phys. Chem. Chem. Phys.* **2006**, *8*, 58 – 62.
[12] V. P. Denysenkov, T. F. Prisner, J. Stubbe, M. Bennati, *Appl. Magn. Reson.* **2005**, *29*, 375 – 384.
[13] V. P. Denysenkov, T. F. Prisner, J. Stubbe, M. Bennati, *Proc. Natl. Acad. Sci. USA* **2006**, *103*, 13386 – 13390.
[14] Y. Polyhach, A. Godt, C. Bauer, G. Jeschke, *J. Magn. Reson.* **2007**, *185*, 118 – 129.
[15] A. Savitsky, A. A. Dubinskii, M. Flores, W. Lubitz, K. Möbius, *J. Phys. Chem. B* **2007**, *111*, 6245 – 6262.
[16] A. D. Milov, A. B. Ponomarev, Y. D. Tsvetkov, *Chem. Phys. Lett.* **1984**, *110*, 67 – 72.
[17] R. E. Martin, M. Pannier, F. Diederich, V. Gramlich, M. Hubrich, H. W. Spiess, *Angew. Chem.* **1998**, *110*, 2993 – 2998; *Angew. Chem. Int. Ed.* **1998**, *37*, 2833 – 2837.
[18] O. Schiemann, T. F. Prisner, *Quat. Rev. Biophys.* **2007**, *40*, 1 – 53.
[19] M. Bennati, T. F. Prisner, *Rep. Prog. Phys.* **2005**, *68*, 411 – 448.
[20] Note that after the rotation $\boldsymbol{R'_d}$, defined as g(radical 2)→D, the D_z axis points from radical 1 towards radical 2 and not vice versa. This fact has to be taken into account when extracting the correct projection angles of radical 2.
[21] P. P. Schmidt, K. K. Andersson, A.-L. Barra, L. Thelander, A. Gräslund, *J. Biol. Chem.* **1996**, *271*, 23615 – 23618.
[22] C. W. Hoganson, G. T. Babcock, *Biochemistry* **1992**, *31*, 11874 – 11880.
[23] P. J. van Dam, J.-P. Willems, P. P. Schmidt, S. Pötsch, A.-L. Barra, W. R. Hagen, B. M. Hoffman, K. K. Andersson, A. Gräslund, *J. Am. Chem. Soc.* **1998**, *120*, 5080 – 5085.
[24] F. Himo, A. Gräslund, L. A. Eriksson, *Biophys. J.* **1997**, *72*, 1556 – 1567.
[25] S. Un, *Magn. Reson. Chem.* **2005**, *43*, S229 – S236.
[26] Note that this definition of dihedral angle as introduced in references [23] and [24] is slightly different but directly related to the more common definition, which uses the location of the H_β protons, C_β, C1, and its p_z axis.
[27] G. Bleifuss, M. Kolberg, S. Pötsch, W. Hofbauer, R. Bittl, W. Lubitz, A. Gräslund, G. Lassmann, F. Lendzian, *Biochemistry* **2001**, *40*, 15362 – 15368.

